Petroleum 1 (2015) 75–81

Contents lists available at ScienceDirect

Petroleum

journal homepage: www.keaipublishing.com/en/journals/petlm

Original article

An experimental study on the internal corrosion of a subsea multiphase pipeline

Shangbi Peng [a, *], Zhaoxiong Zeng [b]

[a] School of Civil Engineering and Architecture, Southwest Petroleum University, Chengdu, China
[b] PetroChina Southwest Pipeline Company, Chengdu, China

ARTICLE INFO

Article history:
Received 14 April 2015
Received in revised form
22 April 2015
Accepted 23 April 2015

Keywords:
Subsea pipeline
Internal corrosion
Experiment
Corrosion inhibitor

ABSTRACT

Based on the actual operational parameters of a subsea multiphase pipeline, an experimental study on the internal corrosion of a subsea multiphase pipeline was conducted in a dynamic, high-temperature autoclave, which had a similar environment to an actual field environment, using the partial pressure of CO_2 (P_{CO2}), velocity of the corrosion medium, temperature, corrosion time, and corrosion inhibitor as variables. The results show that CO_2 resulted in severe localized corrosion and that the corrosion rate increased as the P_{CO2} and velocity increased; the corrosion rate first increased and then decreased with increasing temperature. The corrosion rate peaked at approximately 65 °C and then decreased continuously afterwards; the corrosion rate decreased as the duration of the experimental period increased. Under the operational conditions of the selected subsea pipeline, localized corrosion caused by CO_2 was still the primary corrosion risk. Several types of corrosion inhibitors could inhibit the occurrence of localized corrosion for a short time period; however, most corrosion inhibitors could not completely inhibit localized corrosion.

1. Introduction

As the “lifeline” for the development of offshore oilfields, subsea pipelines play a vital role in the production and transpiration of offshore oil and gas [1]. However, corrosion is a major, hidden danger that threatens the normal operation of subsea pipelines. According to statistics [2], corrosion is the first cause for failure of subsea pipelines.

Between the 1940s and 1950s, many countries began conducting research related to corrosion caused by CO_2. In the 1970s, there was a second upsurge in research that focused primarily on the mechanisms and influencing factors of corrosion [3]. Since then, there has been extensive theoretical and experimental research on the corrosion of subsea pipelines, studies that have primarily focused on the mechanisms of corrosion, prediction of corrosion rates, analysis of the ultimate bearing capacities of corroded pipelines, and the use of corrosion inhibitors in retarding corrosion.

(1) Mechanisms of corrosion and corrosion rates

Based on extensive corrosion data obtained from experiments conducted in laboratories and field monitoring, many petroleum companies and research institutions have proposed a number of different corrosion prediction models, which can generally be classified into three types: empirical models, semi-empirical models, and mechanism models [4–8]. Neural network prediction methods have also been used to predict the corrosion rates of subsea pipelines.

(2) Ultimate bearing capacities of corroded pipelines

Choi et al. [9] conducted an experimental study and a numerical simulation analysis of X65 corroded gas pipelines. Netto et al. [10] studied the effects of the geometric parameters of corrosion and the properties of pipeline materials on the ultimate internal pressure of pipelines through a reduced scale

* Corresponding author.
E-mail address: 254587354@qq.com (S. Peng).
Peer review under responsibility of Southwest Petroleum University.

Production and Hosting by Elsevier on behalf of KeAi

http://dx.doi.org/10.1016/j.petlm.2015.04.003

experiment and a numerical simulation analysis. Pfennig A. [11,12] found that the presence of CO_2 at high temperatures (40–60 °C) considerably corroded steel pipe. Zhang Yucheng et al. [13] researched the relationship between fracture toughness of CO_2 corrosion scale and the corrosion rate of X65 pipeline steel under a supercritical CO_2 condition. Esmaily M. et al. [14] investigated the effect of temperature on the NaCl-induced atmospheric corrosion of Mg–Al alloy AM50 in the laboratory.

(3) Research on corrosion inhibitors

Inhibitors have been primarily applied as individual treatments for corrosion because inhibitors have been proven to be successful and cost effective [15–18]. Inhibitors can act as a surface active component and can form a protective layer on the substrate, modifying the properties of the surface [19,20].

To date, most studies have focused on understanding and quantifying the performance of either corrosion inhibitors or scale inhibitors [21]. R. Ketrane et al. [22] studied the effects of temperature and concentration of five scale inhibitors on calcium carbonate ($CaCO_3$) precipitation from hard water.

In the present study, the actual operational conditions of subsea pipelines were simulated in the laboratory, and the effects of factors such as the partial pressure of CO_2 (P_{CO2}), velocity of the corrosion medium, temperature, corrosion time, and the corrosion inhibitor on the corrosion rate were analyzed under simulated operational conditions. The results of the present study provide a reference for the safe operation of subsea pipelines.

2. Experimental methods

According to the actual operational parameters of subsea pipelines, the corrosion environment of an internal subsea pipeline was simulated in the laboratory. The P_{CO2}, velocity of the corrosion medium, temperature, corrosion time and the corrosion inhibitor were selected as variables.

2.1. Experimental materials and equipment

The failed section of a subsea pipeline that had been recovered from the sea was used as the experimental material. The failed pipeline section was made from X65 pipeline steel, which had the following chemical composition: C $\leq$ 0.26, Si 0.23, Mn $\leq$ 1.45, P $\leq$ 0.03, S $\leq$ 0.03, V + Nb + Ti $\leq$ 0.15, Cr $\leq$ 0.5, Ni $\leq$ 0.5, Mo $\leq$ 0.15, Cu $\leq$ 0.5, and Fe (balance). The main corrosion inhibitors used in the experiment were HYH-151B and C and TS-719B. The medium used in the experiment was the produced liquid from the subsea pipeline. Table 1 lists the composition of the medium.

2.2. Experimental process and steps

The laboratory corrosion simulation was conducted in a dynamic, high-temperature autoclave, which is similar to the actual field environment. The experimental steps were as follows:

Table 1
Composition of the aqueous medium.

Composition	NaCl	$CaCl_2$	$MgCl_2$	$NaHCO_3$
Concentration (g/L)	32.378	1.721	0.431	2.849

(1) The experimental material was machined into specimens with the same shape, which is shown in Fig. 1. The experimental surface of each specimen was polished with 800# abrasive paper. Afterwards, each specimen was degreased and dried with anhydrous ethanol.
(2) After cleaning, each specimen was weighed on an electronic analytical balance with a precision of 0.1 mg. Subsequently, the non-experimental surfaces of each specimen were sealed with 704 silica gel. Then, each specimen was fixed on an experimental fixture, and the superfluous silica gel on the experimental surface was removed with anhydrous ethanol. Each specimen was then placed in a desiccator until the silica gel solidified.
(3) The experimental solution was placed in a deaerator for 24 h to remove the oxygen content with high-purity N_2.
(4) Each specimen was secured on a fixture, which was fixed on a rotary rod inside of the high-temperature autoclave. The solution was then poured into the autoclave. After sealing the autoclave, CO_2 was pumped into the autoclave. The pressure of CO_2 was adjusted when the preset temperature was reached inside of the autoclave. The specimens were rotated at the required speed. During the experimental process, CO_2 was continuously pumped into the autoclave, and the P_{CO2} was maintained. Each group of specimens was removed from the autoclave after the specimens were corroded for 7 d and 30 d. Each specimen was then rinsed with water, degreased with anhydrous ethanol, and dried in cold air. Afterwards, the macroscopic surface morphology of the corrosion product of each specimen was photographed. The corrosion product film on each specimen was removed with acid washing, and then the specimen was rinsed and weighed. The mean corrosion rate was calculated using the weight loss method. The macroscopic corrosion morphology of each specimen, whose corrosion product was removed, was photographed after the specimen was dried in cold air.

3. Experimental results and analysis

3.1. Effect of P_{CO2} on the corrosion rate

Figs. 2 and 3 show the external morphologies and corrosion rates of the internal subsea pipeline (X65 steel) that was corroded under different P_{CO2} values for 30 d, respectively (experimental conditions: temperature, 75 °C; velocity of the corrosion medium, 1.5 m/s; corrosion medium, produced liquid from the recovered pipeline). It can be observed that severe localized corrosion occurred on the surfaces of the specimens under long (30 d) experimental conditions. When other conditions remained the same, the corrosion rate increased when the P_{CO2} increased from 0.3 MPa to 0.5 MPa, which occurred because

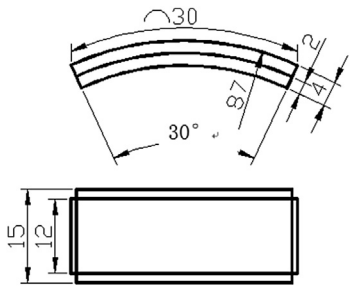

Fig. 1. Material specimen.

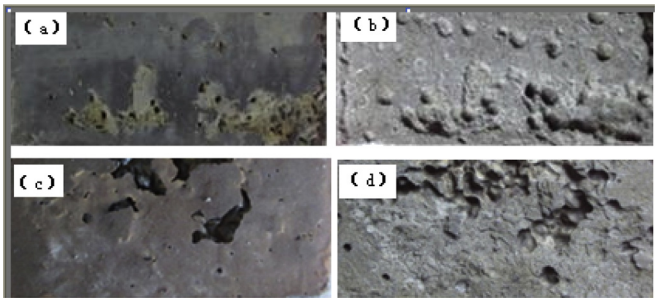

Fig. 2. Morphologies of corrosion specimens under different P_{CO2} values (a) 0.3 MPa (before rust removal); (b) 0.3 MPa (after rust removal); (c) 0.5 MPa (before rust removal); (d) 0.5 MPa (after rust removal).

P_{CO2} affects corrosion primarily by changing the pH of the medium – the higher the P_{CO2} is, the lower the pH is, the faster the depolarization reaction is, and the faster the metal is corroded [1].

3.2. Effect of the velocity of the corrosion medium on corrosion rate

Field observations and studies [8] have shown that the velocity of the corrosion medium significantly impacts internal corrosion. The scouring effect of high-speed water flows can easily destroy corrosion product films or prevent the formation of corrosion production films, affecting the effect of corrosion inhibitors. Generally, the corrosion rate increases with increasing velocity of the corrosion medium. Bruke analyzed the results of the research conducted by Saton, Waard, Ikded, and others and found that the corrosion rate increased rapidly with increasing velocity of the corrosion medium. However, the corrosion rate is not necessarily low when the velocity of the corrosion medium is low. Research has shown that excessively low velocities of the corrosion medium can easily increase localized corrosion rates.

The corrosion rates were measured under different velocities of the corrosion medium (0.7 m/s, 1 m/s, and 1.5 m/s) (experimental conditions: temperature, 60 °C; P_{CO2}, 0.3 Ma; duration of the experimental period: 7 d). Figs. 4 and 5 show the macroscopic morphologies and corrosion rates of the surfaces of the corroded specimens under different experimental conditions.

The experimental results show that the corrosion rate increased when the velocity of the corrosion medium increased from 1 m/s to 1.5 m/s. The primary reasons for the occurrence of such phenomenon are as follows:

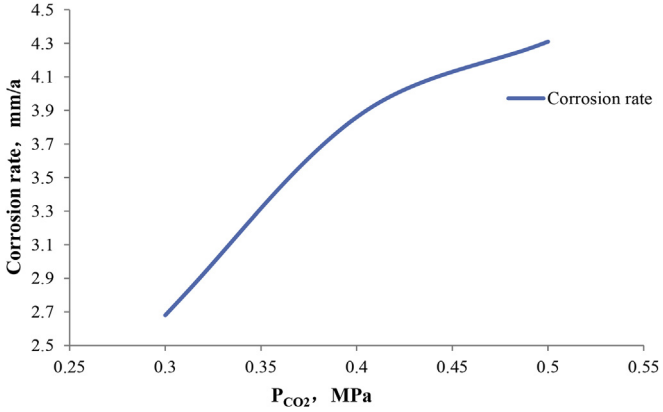

Fig. 3. Effect of P_{CO2} on corrosion rate.

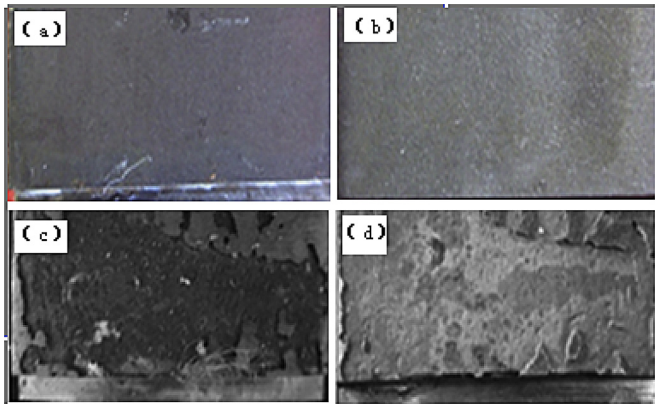

Fig. 4. Morphologies of corroded specimens under different velocities of the corrosion medium (a) 1 m/s (before rust removal); (b) 1 m/s (after rust removal); (c) 1.5 m/s (before rust removal); (d) 1.5 m/s (after rust removal).

(1) The ion transport rate increased as the velocity of the corrosion medium increased, accelerating the corrosion reaction. Therefore, the corrosion rate continuously increased with increasing velocity of the corrosion medium.
(2) After the velocity of the corrosion medium increased, the amount of the corrosion inhibitor that was injected into the pipeline to inhibit corrosion would decrease, and thus, the mitigating effect of the corrosion inhibitor on the corrosion of the pipeline would also weaken, further increasing the corrosion rate of the pipeline.
(3) After the velocity of the corrosion medium increased, the tangential force that the fluid exerts on the inner wall of the pipeline increased; the tangential force prevents the formation of corrosion product films; in addition, the tangential force also has a detrimental effect on the corrosion product films that had already formed.

3.3. Effect of temperature on the corrosion rate

Fig. 6 shows the statistical corrosion results of X65 steel that was corroded in the produced liquid for 7 d under different temperature conditions (experimental conditions: $P_{CO2,}$ 0.3 MPa; velocity of the corrosion medium, 1.0 m/s).

It can be observed that the corrosion rate first increased and then decreased with increasing temperature; the corrosion rate peaked at approximately 65 °C and then continuously decreased

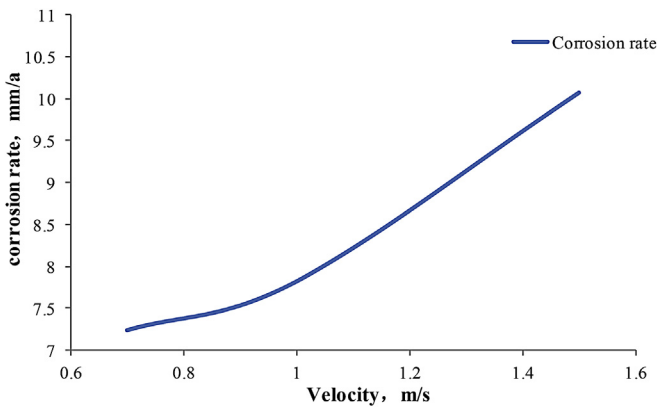

Fig. 5. Effect of the velocity of the corrosion medium on corrosion rate.

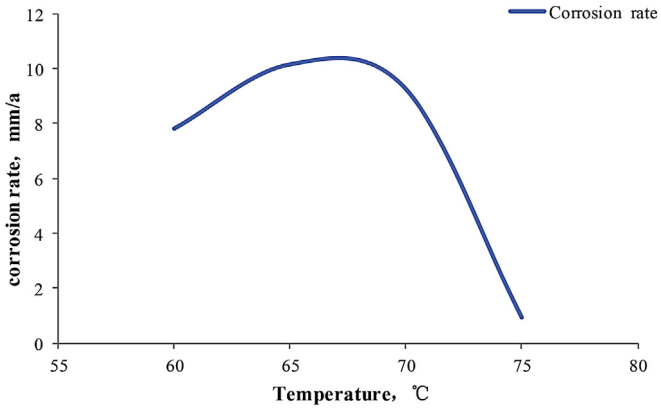

Fig. 6. Effect of temperature on corrosion rate.

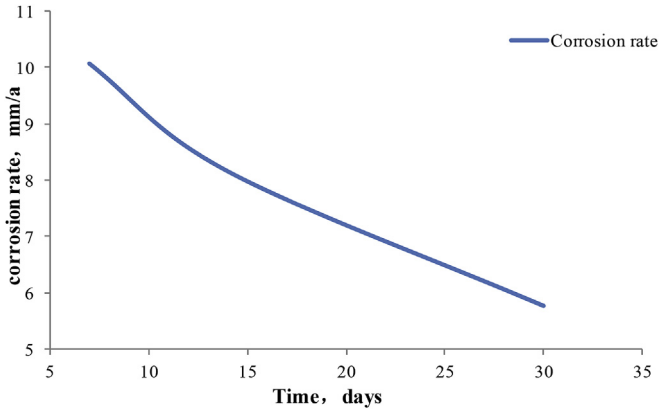

Fig. 7. Effect of the corrosion time on the corrosion effect

afterwards. The primary reasons for the occurrence of such phenomenon of changes in the corrosion rate are as follows:

(1) When the temperature was between 20 °C and 65 °C, the rate of the chemical corrosion reaction continuously increased with increasing temperature. In addition, the amount of the corrosion product films formed on the inner wall of the pipeline was relatively small, and the structure of these corrosion product films was unstable. Thus, these corrosion product films had an insignificant protective effect on the inner wall of the pipeline, and the chemical reaction played the dominant role. Therefore, within the temperature range of 20°C–65 °C, the corrosion rate continuously increased with increasing temperature, and uniform corrosion was the primary corrosion mechanism of the pipeline.

(2) When the temperature was greater than 65 °C, the rate of the chemical corrosion reaction further increased with increasing temperature. However, the structure of the corrosion product films on the inner wall of the pipeline stabilized, and the amount of these corrosion product films continuously increased; thus, the protective effect of these corrosion product films on the inner wall of the pipeline continuously increased, and the protective effect of the corrosion product films played the dominant role. Therefore, when the temperature was greater than 65 °C, the corrosion rate continuously decreased with increasing temperature, and localized corrosion was the primary corrosion mechanism of the pipeline.

In terms of the design conditions of the selected pipeline, the highest corrosion rate (approximately 10 mm/a) occurred at approximately 65 °C.

3.4. Effect of the corrosion time on the corrosion rate

Figs. 7 and 8 show the statistical results of the corrosion rates of X65 steel that was corroded in the produced liquid for different experimental periods (7 d and 30 d) (experimental conditions: temperature, 60 °C; P_{CO2}, 0.3 MPa; velocity of the corrosion medium: 1.5 m/s). It can be observed that the corrosion rate decreased with increasing corrosion time.

3.5. Effect of corrosion inhibitors

Simulations were conducted with different experimental media: the produced liquid alone and the produced liquid

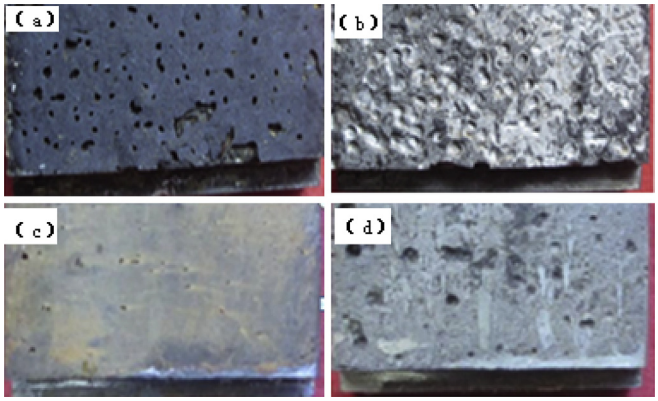

Fig. 8. Corrosion morphologies of specimens under different corrosion times (a) 7d (before rust removal); (b) 7d (after rust removal); (c) 30d (before rust removal); (d) 30d (after rust removal).

combined with a corrosion inhibitor. Simulations were performed for two different experimental periods: a long period (30 d) and a short period (7 d). Table 2 lists the experimental conditions in detail.

(1) Could corrosion inhibitors inhibit localized corrosion?

The long-period (30 d) corrosion experiments were performed in the produced liquid alone (with no corrosion inhibitor added), the produced liquid with 100 ppm of HYH-151B added, and the produced liquid with 100 ppm of C added under the following experimental conditions: temperature, 70 °C; P_{CO2}, 0.3 MPa; and velocity of the corrosion medium: 1.5 m/s. Fig. 9

Table 2
Experimental conditions for the study on the effect of corrosion inhibitors.

Temperature (°C)	CO_2 (MPa)	Velocity (m/s)	Medium	Period (d)
70	0.3	1.5	Produced liquid	30
70	0.3	1.5	Produced liquid +100 ppm HYH-151B	30
70	0.3	1.5	Produced liquid +100 ppm (C)	30
70	0.3	1.5	Produced liquid	7
70	0.3	1.5	Produced liquid +100 ppm HYH-151B	7
70	0.3	1.5	Produced liquid +100 ppm (C)	7
70	0.3	1.5	Produced liquid +100 ppm TS-719B	7

shows the macroscopic morphologies of the specimens that were corroded for 30 d.

It can be observed from Fig. 9 that severe localized corrosion occurred on the surfaces of the specimens that were corroded in the produced liquid with no corrosion inhibitor added under these experimental conditions. Relatively severe platform corrosion occurred on the surfaces of the specimens that were corroded in the produced liquid with 100 ppm of HYH-151B added. The specimens that were corroded in the produced liquid with C added exhibited relatively smooth surfaces, and thus, uniform corrosion was the corrosion mechanism of these specimens.

Fig. 10 shows the corrosion rates of the internal subsea pipeline that was corroded for 30 d under different conditions. It can be observed that there was no significant difference in the corrosion rate between the specimens that were corroded in the produced liquid with a corrosion inhibitor added and the specimens that were corroded in the produced liquid with no corrosion inhibitor added under these experimental conditions, indicating that it is extremely difficult to inhibit localized corrosion that forms in this environment via the injection of a corrosion inhibitor.

Short-period (7 d) corrosion experiments were performed in the produced liquid alone (with no corrosion inhibitor added), the produced liquid with 100 ppm of HYH-151B added, the produced liquid with 100 ppm of C added, and the produced liquid with 100 ppm of TS-719B, under the following experimental conditions: temperature, 70 °C; P_{CO2}, 0.3 MPa; and velocity of the corrosion medium: 1.5 m/s. Fig. 11 shows the corrosion morphologies.

It can be observed from Fig. 11 that uniform corrosion occurred on the surfaces of the specimens that were corroded in the produced liquid with 100 ppm of HYH-151B added and of the specimens that were corroded in the produced liquid with 100 ppm of C added; however, platform corrosion occurred on

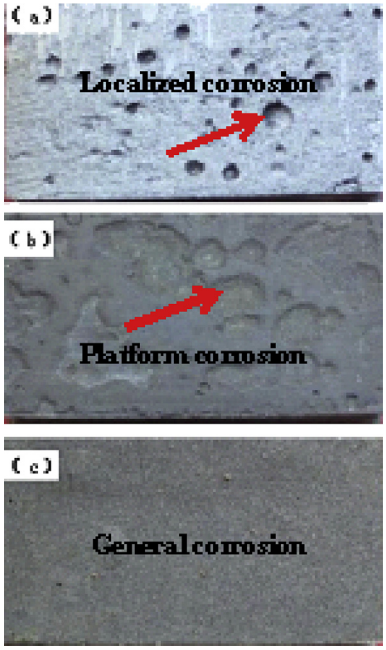

Fig. 9. Macroscopic morphologies of specimens that were corroded for 30 d under different conditions (a) with no corrosion inhibitor added; (b) with a corrosion inhibitor added (100 ppm of HYH-151B); (c) with a corrosion inhibitor added (100 ppm of C).

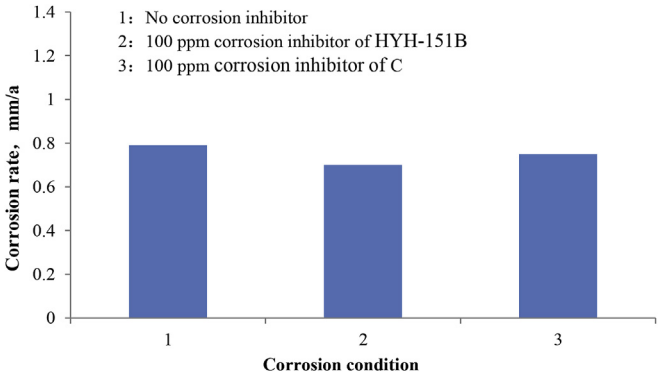

Fig. 10. Corrosion rates of specimens that were corroded for 30 d under different conditions.

several surface areas of the specimens that were corroded in the produced liquid with 100 ppm of TS-719B added.

Fig. 12 shows the corrosion rates of the specimens that were corroded in the produced liquid alone and the specimens that were corroded in the produced liquid with 100 ppm of a corrosion inhibitor added. It can be observed that the corrosion inhibitors had a certain inhibiting effect on corrosion when the specimens were corroded for 7 d; however, there was a relatively large difference in the inhibiting effect among different corrosion inhibitors.

(2) Why did localized corrosion occur?

It can be observed from the macroscopic morphologies of the specimens that were corroded for different times that the corrosion product films were extremely thin when the experiments were conducted for 7 d. The 30-d experimental results show that the corrosion product films were relatively thick, which indicates that the corrosion product films continuously thickened with increasing corrosion time. At 30 d, there were relatively many defects that occurred on the corrosion product films; it was discovered after removing the rust that relatively severe corrosion occurred on essentially all of the defective locations of the corrosion product films, indicating that the occurrence of localized corrosion might be related to the defects of the corrosion product films. Therefore, it can be inferred that localized corrosion was insignificant when the corrosion

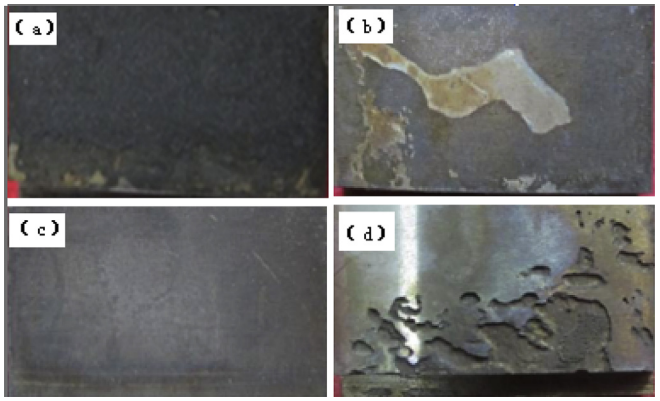

Fig. 11. Macroscopic morphologies of specimens that were corroded for 7 d under different conditions (a) with no corrosion inhibitor added; (b) with a corrosion inhibitor added (100 ppm of HYH-151B); (c) with a corrosion inhibitor added (100 ppm of C); (d) with a corrosion inhibitor added (100 ppm of TS-719B).

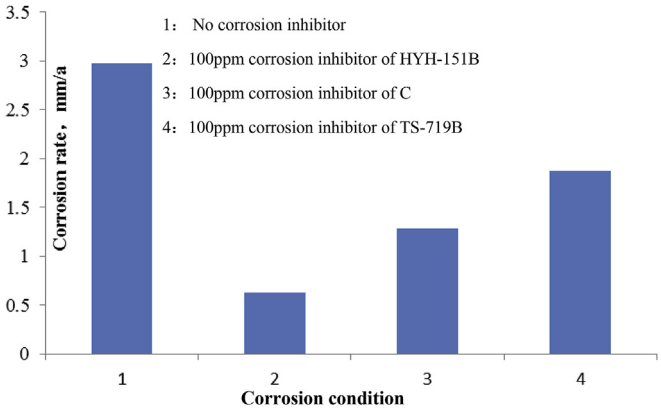

Fig. 12. Corrosion rates of specimens that were corroded in the produced liquid alone and specimens that were corroded in the produced liquid with different corrosion inhibitors added.

experiment was conducted for a relatively short time period, whereas localized corrosion became significant when the corrosion experiment was conducted for a relatively long time period. In addition, the corrosion rate decreased as the duration of the experimental period increased.

The results of the long-period (30 d) corrosion simulation experiments show that the general corrosion rate was approximately 0.8 mm/a, which reflected the conditions of the formation of protective corrosion product films on the inner wall of the pipeline; corrosion inhibitors lost their effect during the 30-d experimental period, and thus, the corrosion rates of the specimens that were corroded in the produced liquid with a corrosion inhibitor added were comparable with those of the specimens that were corroded in the produced liquid with no corrosion inhibitor added. The results of the 7-d experiments show that the corrosion rate was approximately 3–4 mm/a, which was the corrosion rate when fresh metal was exposed due to such reasons as the stripping of the metal and stripping of the scale. The results of the long-period (30 d) corrosion simulation experiments show that the localized corrosion rate of the internal pipeline was greater than 2 mm/a (approximately 2.34 mm/a); the results of the 7-d corrosion simulation experiments show that the localized corrosion rate of the internal pipeline was approximately 8.11 mm/a.

The selected subsea pipeline was located in a sensitive temperature zone of CO_2-induced localized corrosion, in which the aqueous medium had a relatively high salt content and a certain tendency to form scale. According to the results of the simulation experiments performed in the laboratory, localized corrosion of carbon steel can easily occur in such an environment, and it is extremely difficult to inhibit localized corrosion even when injecting corrosion inhibitors.

(3) Important findings

The results of the long-period (30 d) and short-period (7 d) experiments that were performed simultaneously show that due to the characteristics of corrosion development and the important effect of corrosion product films on the corrosion process, relatively high uniform corrosion rates can often be obtained from short-period experiments, and these corrosion rates tend to better reflect the corrosion resistance capacities of steel products and the performances of corrosion inhibitors. The experimental results show that the corrosion rate of the subsea pipeline material was greater than 3 mm/a under the simulated working conditions.

In long-period experiments, corrosion product films are allowed sufficient time to deposit, grow, and become damaged, and etch pits are also allowed sufficient time to form; therefore, the conditions of long-period experiments are closer to those of the field environment. Thus, long-period experiments can reflect the effects of the working field conditions and medium environment on corrosion. Hence, long-period experiments can better reflect the localized corrosion tendency of steel products. The results of the long-period (30 d) experiments clearly show that under the operational conditions of the selected subsea pipeline, localized corrosion caused by CO_2 was still the primary corrosion risk; several types of corrosion inhibitors could inhibit the occurrence of corrosion for a short time period; however, most corrosion inhibitors could not completely inhibit localized corrosion.

4. Conclusions

The relationship between the internal corrosion rate and the factors-P_{CO2}, corrosion mediums, temperature, corrosion time and corrosion inhibitors–is presented. Through the experimental studies, it is concluded that the corrosion rate of the internal subsea pipeline (X65 steel) increased with increasing P_{CO2} and velocity; the corrosion rate first increased and then decreased with increasing temperature – the corrosion rate peaked at approximately 65 °C and then continuously decreased afterwards. The longer the corrosion time was, the higher the corrosion rate was. Under the operational conditions of the selected subsea pipeline, localized corrosion caused by CO_2 was still the primary corrosion risk; certain types of corrosion inhibitor could inhibit the occurrence of corrosion for a short time period; however, most corrosion inhibitors could not completely inhibit localized corrosion. It was extremely difficult to inhibit the localized corrosion that formed in the operational environment of the selected subsea pipeline via the injection of corrosion inhibitors.

Acknowledgment

This paper is a project supported by the Special Fund of China's Central Government for the Development of Local Colleges and Universities——the Project of National First-level Discipline in Oil and Gas Engineering.

References

[1] X. Zhang, A Study on the Ultimate Bearing Capacities and Failure Mechanisms of Corroded Subsea Pipelines, Zhejiang University, 2013.
[2] MMS, Proceeding of the International Workshop on the Damage to Underwater Pipelines, Minerals Management Service, New Orleans, USA, 1995.
[3] F. Liu, A Study on the Corrosion Patterns as Well as the Corrosion Properties and Mechanisms of the Drilling Tool-pipeline System for Oilfields, A master's dissertation from Ocean University of China, 2008.
[4] G. Yang, G. Liang, Analysis of the corrosion of the downhole oil pipelines in the Yakela-Dalaoba gas condensate field, Corros. Prot. 32 (12) (2011) 1001–1008.
[5] Anon, CO2 corrosion Rate Calculation Model, Norway, 2005.
[6] C. De Warrd, U. Lotz, A. Dugstad, NACE, Influence of Liquid Flow Velocity on CO_2 Corrosion : a Semi-empirical Model, 128, Corrosion 95, Houston, TX, 1995.
[7] X. Li, A Study on the Corrosion of Downhole Oil Pipelines Caused by Carbon Dioxide, A master's dissertation from Sichuan University, 2005.
[8] J. Zhou, Corrosion Behavior of Casing Steel in a High-temperature High-pressure CO_2 and H_2S-containing Aqueous Medium and Functions of Protection Technologies, Northwestern Polytechnical University (Xi'an), 2002.
[9] J.B. Choi, B.K. Goo, J.C. Kim, W.S. Kim, Development of limit load solutions for corroded gas pipelines, Int. J. Press. Vessels Pip. 80 (2003) 121–128.

[10] T.A. Netto, U.S. Ferraz, S.F. Estefen, The effect of corrosion defects on the burst pressure of pipelines, Int. Constr. Steel Res. 64 (2005) 1185–1204.
[11] A. Pfennig, A. Kranzmann, Effects of saline aquifer water on the corrosion behaviour of injection pipe steels 1.4034 and 1.7225 during exposure to a CO_2 environment, Energy Proc. 1 (2009) 3023–3029.
[12] A. Pfennig, B. Linke, A. Kranzmann, Corrosion behavior of pipe steels exposed for 2 years to CO_2-saturated saline aquifer environment similar to the CCS site Ketzin, Ger. Energy Proc. 4 (2011) 5122–5129.
[13] Zhang Yucheng, Pang Xiaolu, Qu Shaopeng, The relationship between fracture toughness of CO_2 corrosion scale and corrosion rate of X65 pipeline steel under supercritical CO_2 condition, Int. J. Greenh. Gas Control 5 (6) (2011) 1643–1650.
[14] M. Esmaily, M. Shahabi-Navid, J. Svensson, et al., Influence of temperature on the atmospheric corrosion of the Mg-Al alloy AM50, Corros. Sci. 90 (2015) 420–433.
[15] Md Shamsuddoha, Md Mainul Islam, Thiru Aravinthan, et al., Effectiveness of using fibre-reinforced polymer composites for underwater steel pipeline repairs, Compos. Struct. 100 (2013) 40–54.
[16] L. Garverick, Corrosion in the Petrochemical Industry, ASM International, Materials Park, OH, 1994.
[17] G.V. Chilingar, R. Mourhatch, G.D. Al-Qahtani, Fundamentals of Corrosion and Scaling - for Petroleum and Environmental Engineers, Gulf Publishing Company, Houston, Texas, 2008.
[18] Laura Sanders, Xinming Hu, Eleftheria Mavredaki, et al., Assessment of combined scale/corrosion inhibitors - A combined jar test/bubble cell, J. Petroleum Sci. Eng. 118 (2014) 126–139.
[19] S. Nesic, R. Nyborg, M. Nordsveen, A. Stangeland, Mechanistic Modeling for CO2 Corrosion with Protective Iron Carbonate Films NACE International, Houston, TX, 2001. CORROSION 2001.
[20] W. Sun, S. Nesic, kinetics of corrosion layer formation: part 1 – iron carbonate layers in carbon dioxide corrosion, Corrosion 64 (4) (2008) 334–346.
[21] X. Hu, R. Barker, A. Neville, A. Gnanavelu, Case study on erosion–corrosion degradation of pipework located on an offshore oil and gas facility Wear 271 (9–10) (2011) 1295–1301.
[22] R. Ketrane, B. Saidani, O. Gil, L. Leleyter, F. Baraud, Efficiency of five scale inhibitors on calcium carbonate precipitation from hard water: effect of temperature and concentration, Desalination 249 (3) (2009) 1397–1404.